Rev.Adv.Mater.Sci. 25 (2010) 52-57

STRUCTURE AND PROPERTIES OF NANOCRYSTALLINE ALLOYS PREPARED BY HIGH PRESSURE TORSION

A. Aronin, G. Abrosimova, D. Matveev and O. Rybchenko

Institute of Solid State Physics RAS, Chernogolovka, Moscow Distr., Russia

Received: November 11, 2009

Abstract. Formation of nanocrystalline structure in amorphous Fe-B-Si alloy under severe plastic deformation was studied by X-ray diffraction and transmission electron microscopy. Severe plastic deformation of the alloy has been carried out by high pressure torsion method with a pressure of 4 GPa. The severe plastic deformation was found to lead to an appearance of Fe(Si) nanocrystals in the amorphous matrix. The nanocrystal size is independent of the deformation level and they formed by diffusion mechanism of crystallization. When the deformation degree increases, the volume fraction of the nanocrystalline phase also increases. The average size of the nanocrystals formed at severe plastic deformation was found to depend on the deformation temperature. The nanocrystalline phase formation may lead to increase saturation magnetization.

1. INTRODUCTION

Nanocrystalline materials are currently an active area of research, as they have an unusual structure and, consequently, unique physical and chemical properties. The formation, evolution and decomposition of such structure as well as the structure/property correlation are of a special interest [1,2]. One of the widely used methods to create nanocrystals is controlled crystallization of the amorphous phase. After completion of the first stage of crystallization the structure is usually two-phase and consists of nanoparticles of a single crystalline phase embedded in the amorphous matrix [3]. One of the first alloys, Fe-Si-B-Cu-Nb, known as FINEMET, exhibits superior soft magnetic properties with low coercivity (0.5 – 1 A/m) and high saturation magnetization exceeding 1.4 T [4]. This alloy is based on widespread amorphous Fe-Si-B alloys with addition of a small amount of copper (1%) and niobium (3%). However, the resulting sample thickness of such alloys prepared as ribbons is usually less than 50 μm. The dimension limit restricts the use of these materials in a number of potential applications. Furthermore, the presence of expensive niobium and copper in the alloy deteriorates the soft magnetic properties of Fe-based alloys decreasing saturation magnetization of the samples.

Therefore, a new splash of interest to nanocrystalline materials with high magnetic properties is connected with the development of the severe plastic deformation (SPD) method [5-7]. This method enables creation of nanocrystalline structure in bulk materials and in alloys that cannot be prepared as nanocrystalline by annealing. Nanocrystalline structure can be formed under SPD both at room and higher temperatures [6]. The important point of nanocrystallization under SPD is the change of the sequence of phase formation as compared with crystallization of the amorphous phase on heating [8]. The α-Fe or Fe(Si) solid solution nanocrystals were found to form under SPD even in Fe-B and Fe-Si-B alloys of hypereutectic composition.

The aim of the present work is to study the dependence of volume fraction of nanocrystalline phase

Corresponding author: A. Aronin, e-mail: aronin@issp.ac.ru

and the magnetic properties on the level and temperature of severe plastic deformation of $Fe_{81}Si_{13}B_6$ amorphous alloy. This is a basic alloy for nanocrystalline FINEMET but containing no copper and niobium. The nanocrystalline structure cannot be formed by controlled crystallization of this alloy.

2. EXPERIMENTAL METHODS

Amorphous $Fe_{81}Si_{13}B_6$ alloy was prepared by melt quenching. Severe plastic deformation of the alloy was carried out by the high pressure torsion method (HPT) [9] at a pressure of 4 GPa. After the deformation the samples were disc-shaped; the diameter and the thickness of the discs were 3 mm and 0.24 mm, respectively. The sample was placed between two anvils and the upper anvil rotated.

The true logarithmic extent of the deformation was determined as $\varepsilon = \ln(\Theta r/l)$, where Θ is the rotation angle of the anvil in the radian, r the sample radius, l the disc thickness. The extent of the deformation was $4.5 \div 5.05$ in the middle part of the sample radius. The deformation was carried out at 20 °C.

The structure of the samples was studied by X-ray diffraction and transmission electron microscopy. The X-ray diffraction (XRD) measurements were performed on a SIEMENS D-500 diffractometer with Fe K_α radiation. Special computer programs were used for processing the X-ray diffraction spectra (smoothing, background correction, *etc*.). At the early crystallization stages, the samples contained amorphous and nanocrystalline phases when separation of the overlapped peaks was carried out. The data on the position and halfwidth of diffuse halo of the initial amorphous phase were taken into account. The nanocrystal size was determined both by the dark field electron microscopy images and the XRD data.

The size of the nanocrystals was determined both by the dark filed electron microscopy images and the X-ray diffraction pattern. In the latter case Scherrer formula [10] was used:

$$L = \lambda \frac{1/\cos\theta}{\Delta(2\theta)}, \qquad (1)$$

where L is the nanocrystals size, λ the radiation wavelength, θ the diffraction angle, $\Delta(2\theta)$ the halfwidth of the reflection.

The halfwidth of the reflections consists of two parts connected with the sample and the collimation system (instrumental halfwidth). In order to determine true halfwidth β_s, the Kauchi or Gauss relation is commonly used [10]:

$$\beta_s^2 = \beta_{exp}^2 - \beta_{st}^2, \qquad (2)$$

where β_{exp} is the value of the halfwidth obtained from the XRD data and β_{st} is a value of the halfwidth of the standard obtained for the used collimation system. However, the halfwidth of the reflections is large for the nanocrystalline phase and the instrumental halfwidth can be neglected.

The microstructure was studied by transmission electron microscopy using a JEM-100CX electron microscope. The spots located at 0.2-1 mm from the center of the samples were studied.

The measurements of the magnetic properties were carried out at room temperature using a vibration magnetometer.

3. RESULTS

After the preparation the ribbons were amorphous (Fig. 1). The electron and X-ray diffraction patterns contained only wide halos typical for the amorphous phase; the reflections from crystalline phases were not observed.

Severe plastic deformation leads to crystallization of the amorphous phase. The structure consists of an amorphous phase with randomly arranged nanocrystals. The reflections in the XRD patterns correspond to BCC structure with lattice parameter a = 0.2866 nm. They may belong both to the α-Fe and Fe_3Si phase, but the date obtained are insufficient to make a conclusion about the phase formed.

The electron microscopy micrograph (Fig. 2) shows that the nanocrystals occupy a noticeable part of the sample.

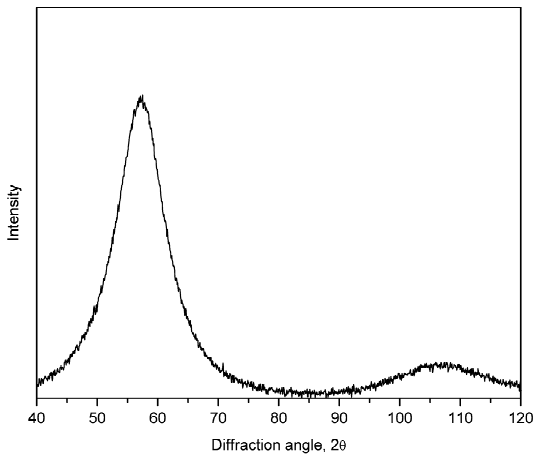

Fig. 1. XRD pattern of as-prepared amorphous sample.

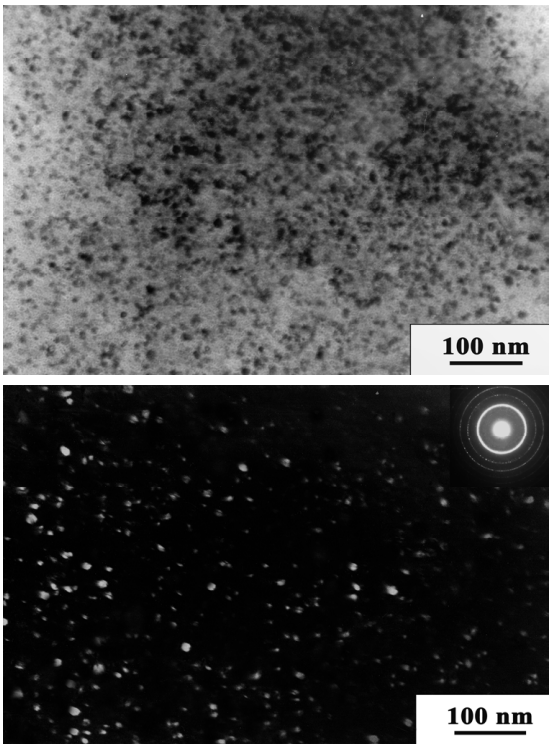

Fig. 2. TEM image of as-deformed structure: (a) bright field image and (b) dark field image in part of the first ring of electron diffraction pattern.

The nanocrystals are distributed in the amorphous matrix, their size determined by dark field images is 5-15 nm. Since transmission electron microscopy is a local method, the X-ray data were used to determine the average size of the nanocrystals in the sample.

As mentioned above, in the case of co-existence of amorphous and nanocrystalline phases the overlapped peaks in the XRD patterns should be separated. Figs. 3a-3c show separation of the parts of the XRD patterns for the as-prepared sample (Fig. 3a) and the samples after SPD using 8 (Fig. 3b) and 15 (Fig. 3c) rotations. The parameters of the main diffuse halo (the position and the halfwidth of the diffuse peak) of the as-prepared amorphous alloy were taken into account when separating the XRD patterns of the deformed samples.

The peaks in the X-ray patterns were approximated by the Gauss functions, the parameters obtained for the initial amorphous phase (Fig. 3a) were used as start values in the decomposition of the peaks in the diffraction patterns of the deformed samples. It is significant that the experimentally obtained maxima shown in Figs. 3b and 3c cannot be described by a single Gaussian which unam-

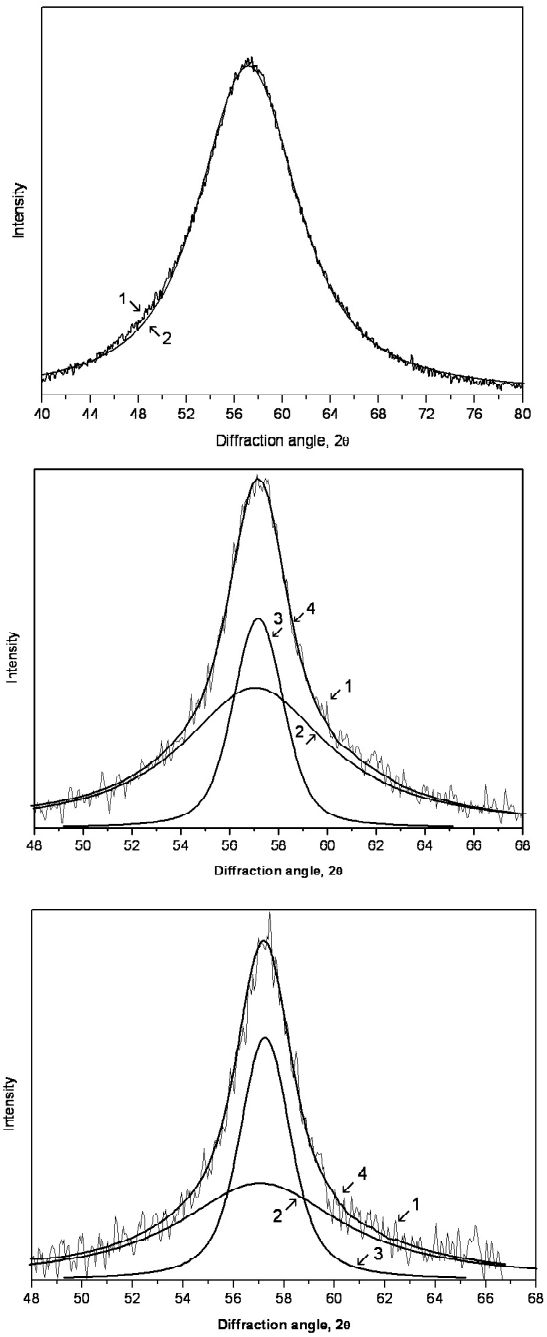

Fig. 3a. Part of XRD pattern shown in Fig 1*a*: experimental (1) and calculated curves for amorphous phase (2). **b.** XRD pattern of samples after 8 rotation SPD: experimental (1) and calculated curves for amorphous phase (2), crystalline phase (3) and sum of amorphous and crystalline contributions (4). **c.** XRD pattern of samples after SPD for 15 rotations: experimental (1) and calculated curves for amorphous phase (2), crystalline phase (3) and sum of amorphous and crystalline contributions (4).

biguously points to an extra contribution to the intensity. The curves in Figs. 3b and 3c correspond to the experimental data (1) and the calculated curves to the amorphous phase (2), the crystalline phase (3) and the sum of the amorphous and crystalline contributions (4). It should be noted that the curves corresponding to the amorphous phase in Figs. 3b and 3c have the same angle position and different intensity which manifests itself as the change of the volume fraction of the amorphous (and crystalline) phase under the deformation.

Upon decomposition it was assumed that the curve of scattering from the amorphous phase remains unchanged while the intensity value can vary, thereby reflecting the part of the amorphous phase in the sample. Strictly speaking, this is not exactly correct since the structure of the amorphous phase can change at the expense of structural relaxation as well as during deformation. It is known, however, that the changes of the scattering curve occurring on relaxation are insignificant (the intensity of the first maximum increases by 2-3%, whilst the change of the halfwidth is negligible [11,12]) that are essentially smaller than those observed. Besides, the deformation was carried out at room temperature, hence, the relaxation processes can be neglected. Figs. 3b and 3c show that the halfwidth of the halo decreases appreciably (from 6.3 (in 2Θ units, Fe radiation) to 1.76) and during decomposition the integral intensity of the extra maximum corresponding to the nanocrystalline phase makes up approximately half of the whole intensity maximum.

Obviously, the severe distortion of the shape of the diffusion maximum cannot be also caused by the above changes of the amorphous structure. For instance, multiple rolling of amorphous $Pd_{40}Ni_{40}P_{20}$ alloy [13] resulted in anisotropy of X-ray scattering (shift of the diffuse maximum lengthwise and transverse to the deformation direction) without significant change of its halfwidth. Yet, the experiments with $Zr_{30}Cu_{60}Ti_{10}$ alloy revealed [14], that formation of even extremely small nanocrystals 1-5 nm in size results in the change of the halfwidth of the diffusion maximum (from 4.3 (in 2Θ units, Cu radiation) down to 3.6) which is indicative of an extra contribution to the scattering induced by nanocrystals.

Therefore, the shape of reflection changes under deformation. As this takes place, the halfwidth of the reflections from the crystalline phase in both deformed samples is the same, its value corresponding to the nanocrystalline structure. The size of the nanocrystals determined by the Sherrer formula is 8 nm for both levels of the deformation. In contrast, the integral intensities of the reflections are different and increase with the deformation level. This means that the volume fraction of the nanocrystalline phases increases under deformation. The deformation of 15 rotation leads to increasing volume fraction of the nanocrystalline phase as compared with the deformation of 8 rotations while the nanocrystal size remains unchanged. The nanocrystal size is also the same in the samples deformed by 10 rotations and the volume fraction of the nanocrystalline phase varies from 8 to 15 rotations. The nanocrystal size is independent of the deformation level and the nanocrystals form by the diffusion mechanism of crystallization since the composition of the nanocrystals and initial amorphous phase are different.

Precise determination of the value of the volume fraction of the phases by the XRD data shown in Fig. 3 is complicated since the reflections from the nanocrystalline phase are result of diffraction and diffuse halo from the amorphous phase is result of scattering. However, the square under the reflection from the nanocrystalline phase is significantly larger than that under the diffuse halo and one may expect that the volume fraction of the nanocrystalline phase is more than one half of the sample, which is in agreement with the data of electron microscopy.

The independence of the average size of nanocrystals induced by deformation in amorphous $Fe_{81}Si_{13}B_6$ alloy from the value of deformation can be due to several factors. First, as in [15], it can be assumed that having reached a critical size the nanocrystals undergo plastic deformation resulting in their fragmentation. The phenomenon was observed in amorphous $Al_{88}Y_7Fe_5$ alloys crystallized under SPD [15,16]. It was observed [15,16] that the maximum size of deformation-induced Al nanocrystals does not exceed 15-18 nm, although the deformation varies over a wide range. Therefore, the maximum size of deformation-induced nanocrystals appears to be largely independent of the strain level. It is assumed that nanocrystals exceeding a critical size and subjected to further deformation can show a plastic deformation behavior and eventually break during continuous deformation. Observation of dislocations in one of the nanocrystals suggests a shear-induced fragmentation mechanism [16]. Similar occurrence of dislocations and fragmentation of 20 nm-sized nanocrystals we observed in HPT-induced amorphous Fe-B alloys.

Second, it should be noted that nanocrystals form by the diffusion mechanism (the primary crystallization reaction) and their composition is different from that of the initial amorphous phase. There-

fore, in principle, it can be expected that nanocrystal growth is severely limited by this extremely high number density due to the earlier overlapping diffusion fields. However, in $Fe_{81}Si_{13}B_6$ alloy the nanocrystals make Fe(Si) solid solution, hence, there is boron rather than silicon redistribution in front of the reaction front. Since the boron diffusion constant is fairly high and the boron content in the alloy insignificant, this process may have no appreciable effect on the size of nanocrystals. Therefore, changes in the composition of the amorphous matrix (boron enrichment) during Fe(Si) nanocrystal growth are unlikely to limit the growth of nanocrystals even at their concentration exceeding 50%. To change the type of reaction, far more significant boron enrichment of the matrix is required (the eutectic point in Fe-B alloys corresponds to 17.5 at.% B). It is well known that in alloys of the same composition, but with admixture of copper (1%) and niobium (3%) (FINEMET), the growth of nanocrystals during thermal treatment is controlled by diffusion of niobium, the amount of the nanocrystalline phase being 70-80%.

Third, the independence of the average size of nanocrystals from the deformation value can be related to the fact that increasing deformation involves an increased number of shear bands wherein deformation occurs, i.e. delocalization of deformation is observed. As is known, in the case of uniaxial tension deformation takes place over a shear bands whereas plastic deformation under multiaxial stress involves intersection and branching of shear bands [17]. Intersection of shear bands slows down further deformation along the pre-formed shear band. Subsequent deformation generates new shear bands in the undeformed amorphous matrix. Such deformation mechanism is responsible for the fixed size of nanocrystals. If deformation always takes place in new region of the sample, the nucleation and growth of nanocrystals in the new sites are similar to those in the previous sites and, as a result, nanocrystals will grow to the same size.

The formation of a large fraction of the crystalline phase should lead to a change of the magnetic properties of the samples.

Saturation magnetization, M_s, of amorphous alloys is known to be less than that of crystalline alloys or iron, hence, substitution of part of the amorphous phase by a crystalline phase should increase saturation magnetization. Fig. 4 shows the hysteresis loops for as-prepared (amorphous) and SPD-deformed (amorphous-crystalline) samples. The value of M_s is about 180 EMU/g in the as-prepared amorphous alloy. The formation of the nanocrystalline phase leads to an increase of ~ 10% of M_s. The coercivity of the deformed sample is about 1 Oe. This value is about 20% higher than the coercivity of the as-prepared amorphous sample.

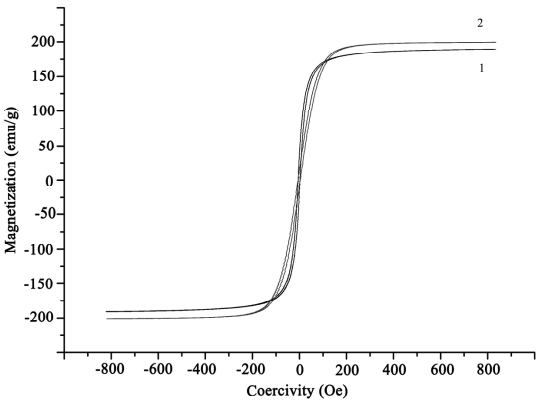

Fig. 4. Hysteresis loops for as-prepared sample and (1) and sample deformed 10 rotations (2).

The key factor for understanding the relationship between the magnetic properties and the microstructure is analysis of magnetic anisotropies and how they can be controlled. Coercivity, H_c, increases with anisotropy energy density, K, as [18].

$$H_c = \frac{p_c < K >}{M_s}, \qquad (3)$$

where M_s is the average saturation magnetization of the material and, p_c is the dimensionless pre-factors close to unity.

The basic anisotropy contributions are (i) magneto-crystalline anisotropy, K_1, (ii) magneto-elastic anisotropy, K_y, and (iii) stress induced anisotropies, K_u. The magnetic softening of nanocrystalline ferromagnets is due to the suppression of the local magneto-crystalline anisotropy by the exchange interaction [19]. The mechanism becomes effective for grain sizes, D, smaller than the ferromagnetic exchange length, $L_0 = (A/K_1)^{0.5}$ (A is the exchange stiffness and K_1 is the magneto-crystalline anisotropy constant). In our case, the average crystal size is 8 nm (Fe(Si) nanocrystals) and L_0 = 35 nm; and $L_0 \approx 2 \times 10^3$nm for the two phase system (amorphous phase + Fe(Si) nanocrystals) [19].

In order to improve the soft magnetic properties, other components of the anisotropy should be also decreased. In particular, the low magnetostriction constant is expected to minimize magneto-elastic

anisotropies. The saturation magnetostriction, λ_s, determines magneto-elastic anisotropies $K_s = -3/2\ \lambda_s\sigma$ (σ is internal or external mechanical stress). The phases formed on crystallization of nanocrystalline Fe-base alloys lead to low λ_s, which minimizes the magneto-elastic anisotropy.

It should be noted that the positive magnetostriction of the residual amorphous phase can be balanced by the negative magnetostriction of the nanocrystalline phase in the alloys of the FINEMET type. However, the total balance may be realized when the volume fracture of the Fe(Si) nanocrystals is 70 – 80%. In our case the content of the nanocrystalline phase can be less and no total balance may be realize. Another reason for increasing coercivity may be connected with the anisotropy induced by the deformation. The appearance of such anisotropy also leads to a change of the hysteresis loop shape after the SPD deformation in comparison with the as-prepared amorphous sample.

Thus, the nanocrystalline structure consisted of BCC nanocrystal Fe(Si) solid solution is distributed in the amorphous phase that was formed in the amorphous $FeSi_{13}B_9$ alloy by severe plastic deformation. Following deformation the fraction of the nanocrystalline phase exceeds 50%, the average size of the nanocrystals being 8 nm. The volume fraction of the nanocrystals increases with increasing deformation level while the nanocrystal size remains unchanged. The nanocrystalline phase formation can lead to increase of the saturation magnetization.

ACKNOWLEDGEMENTS

The authors are grateful to the RBRF (projects 09-02-00529 and 07-02-00424) for the financial support.

REFERENCES

[1] A.R. Yavari and O. Drbohlav // *Mater. Trans. JIM* **36** (1995) 896.
[2] Y. Yoshizawa // *Mater. Sci, Forum* **307** (1999) 51.
[3] G.E. Abrosimova, A.S. Aronin, Yu.V. Kir'janov, I.I. Zver'kova, V.V. Molokanov, H. Alves and U. Koster // *J. Mater. Sci*. **34** (1999) 1611.
[4] Y. Yoshizawa, S. Oguma and K. Yamauchi // *J. Appl. Phys*. **64** (1988) 6044.
[5] N. Noskova, L. Korshunova, A. Potapov and N. Tchernenko, In: *Investigations and applications of severe plastic deformation*, ed. by T.C. Lower and R. Z. Valiev (2000), p.115.
[6] D.V. Gunderov, A.G. Popov, N.N. Scheglova, V.V. Stolyarov and A.R. Yavary, In: *Nanomaterials by Severe Plastic Deformation*, ed. by M.J. Zehetbuuer and R.Z. Valiev (2004), p.165.
[7] R.Z. Valiev, In: *Nanomaterials by Severe Plastic Deformation*, ed. by M.J. Zehetbuuer and R.Z. Valiev (2004), p.109.
[8] G.E. Abrosimova, A.S. Aronin. S.V. Dobatkin, I.I. Zverkova, D.V. Matveev, O.G. Rybchenko and E.V. Tatyanin // *Solid State Physics* **49** (2007) 983.
[9] R.Z. Valiev and I.V. Aleksandrov, *Nanostructure materials obtained by severe plastic deformation* (Logos, Moscow, 2000).
[10] A. Guinier, *Theorie et technique de la radiocristallographie* (Dumond, Paris, 1956).
[11] T. Masumoto, X. Waseda, H. Kimura and A. Inoue // *Sci. Rep. RITU* **26A** (1976) 21.
[12] V.V. Nemoshkalenko, A.V. Romanova and A.G. Iliinsky // *Amorphous metallic alloys* (Naukova dumka, Kyiv, 1987).
[13] G. Abrosimova, A. Aronin, N. Afonikova and N. Kobelev // submitted in *Solid State Physics.*
[14] A.S. Aronin, G.E.Abrosimova, A.F.Gurov, Yu.V. Kir'yanov and V.V.Molokanov // *Mater. Sci. Eng.* **A304-306** (2001) 375.
[15] N. Boucharat, R.J.Hebert, H. Rösner, R. Valiev and G. Wilde // *Scr. Mater.* **53** (2005) 823.
[16] R.J. Hebert, J.H. Perepezko, H. Rösner and G. Wilde // *Scr. Mater.* **54** (2006) 25.
[17] K. Suzuki, H. Fujimori and K. Hashimoto, *Amorphous Metals* (Butterworths, London, 1983).
[18] G. Herzer // *IEEE Trans .Magn.* **26** (1990) 1397.
[19] G. Herzer // *JMMM* **112** (1992) 258.